International Journal of Pharmaceutics 393 (2010) 143–151

Contents lists available at ScienceDirect

International Journal of Pharmaceutics

journal homepage: www.elsevier.com/locate/ijpharm

Preparation and pharmacodynamics of stearic acid and poly (lactic-co-glycolic acid) grafted chitosan oligosaccharide micelles for 10-hydroxycamptothecin

Yue-Yu Zhou [a,b], Yong-Zhong Du [b], Ling Wang [b], Hong Yuan [b], Jian-Ping Zhou [a,**], Fu-Qiang Hu [b,*]

[a] Department of Pharmaceutics, China Pharmaceutical University, 24 Tongjiaxiang Road, Nanjing 210009, PR China
[b] College of Pharmaceutical Science, Zhejiang University, 388 Yuhangtang Road, Hangzhou 310058, PR China

ARTICLE INFO

Article history:
Received 3 March 2010
Received in revised form 8 April 2010
Accepted 19 April 2010
Available online 24 April 2010

Keywords:
Stearic acid
Chitosan oligosaccharide
PLGA
Polymeric micelle
10-Hydroxycamptothecin
Anti-tumor

ABSTRACT

Stearic acid (SA) and poly (lactic-co-glycolic acid) (PLGA) grafted chitosan oligosaccharide (SA-CSO-PLGA SCP) tripolymer was synthesized via the reaction between the carboxyl group of SA or PLGA with carboxylic side group, and the amine group of CSO in the presence of 1-Ethyl-3-(3-dimethylaminopropyl) carbodiimide (EDC). The degrees of amino-substitution for SA and PLGA were assayed through 2, 4, 6-trinitrobenzene sulfonic acid (TNBS) test and ^{13}C NMR spectrum, which were 8.15% and 5.82%, respectively; the critical micelle concentrations of SCP in PBS (pH 7.4) and deionized water (DI water) were about 34.9 and 14.5 μg/ml, respectively. Using 10-hydroxycamptothecin (HCPT) as a model drug, the drug-loaded micelles showed above 86% encapsulation efficiency, which not only enhanced the solubility of HCPT in aqueous medium markedly, but also protected the lactone ring of HCPT. Cellular uptakes of SCP micelles against A549, MCF-7 and HepG-2 tumor cells showed a faster cellular internalization. Comparing to the commercial HCPT injection, HCPT-loaded micelles showed higher cytotoxicities against A549, MCF-7 and HepG-2 cells. The increased folds were 22, 18 and 15, respectively. These results suggested the SCP could be applied as a carrier for hydrophobic drugs.

1. Introduction

Camptothecin (CPT) is a natural indole alkaloid extracted from a Chinese tree Camptotheca acuminate (Nyssaceae) in the 1960s (Wall et al., 1966). Due to the promising and potential anti-tumor activity, CPT and its derivatives including 10-hydroxycamptothecin (HCPT), 9-nitro-camptothecin, topotecan and irinotecan, have attracted more and more attention recently. The anti-tumor mechanism of these compounds is based on the inhibition of DNA replication and RNA transcription by stabilizing the cleavable complexes formed between topoisomerase I and DNA (Tsao et al., 1993; Laco et al., 2002). HCPT has shown the best anti-tumor effect among its analogues and less toxicity in vivo compared with CPT (Han, 1994). It has been widely used in the treatment of gastric carcinoma, hepatoma, leukemia, lung carcinoma and tumor of head and neck in clinic (Zhang et al., 1998; Pourquier and Pommier, 2001; Thomas et al., 2004).

All the CPT analogues can exist in two conformations: the carboxylate form (ring-opened form, O-HCPT) and lactone form (ring-closed form, C-HCPT). It is widely reported that the inhibitory effect of the lactone form on topoisomerase I is higher than that of the carboxylate form (Wani et al., 1980). The integrity of this lactone ring is very important to drug's passive diffusion into tumor cells and suppressing topoisomerase I activity. The lactone ring is stable at pH 6 or lower, but it can be opened rapidly and changed into carboxylate form under alkaline condition (Shenderova et al., 1997). Unfortunately, drug in its active lactone form has a poor solubility in water and physiologically acceptable organic solvents, and its lactone ring readily opened and was converted into the carboxylate form under physiologic and alkaline condition (Fig. 1, Zhang et al., 2007b). Due to the poor solubility of the lactone form, HCPT is usually used in the more soluble form of carboxylate salt which is more toxic and less active (Muggia et al., 1972). In addition, the poor compliance caused by irritation due to alkali limits the application of HCPT.

In order to develop high performance drug delivery systems for the insoluble lactone form of HCPT, many attempts have been made, such as polymer microshperes (Ertl et al., 1999; Zhang et al., 2006; Shenderova et al., 1997; Shenderova et al., 1999; Lu and Zhang, 2006), liposomes (Zhang et al., 2004; Cortesi et al., 1997), emulsions (Cortesi et al., 1997; Zhao et al., 2007), nanoparticles (Sun et al., 2004; Zhang et al., 2006, 2007a; Yang et al., 2007; Guo et al., 2007), niosomes (Shi et al., 2006; Hong et al., 2009) and prodrugs (Carbonero and Supko, 2002; O'Leary and Muggia, 1998; He et al., 2004; Wang et al., 2005). However, these delivery systems still have some obvious limitations, such as low drug loading capacity, adverse effects induced by excipients or sol-

* Corresponding author. Tel.: +86 571 88208439; fax: +86 571 88208439.
** Corresponding author. Tel.: +86 25 83271272; fax: +86 25 83301606.
E-mail addresses: zhoujpcpu@126.com (J.-P. Zhou), hufq@zju.edu.cn (F.-Q. Hu).

0378-5173/$ – see front matter © 2010 Elsevier B.V. All rights reserved.
doi:10.1016/j.ijpharm.2010.04.025

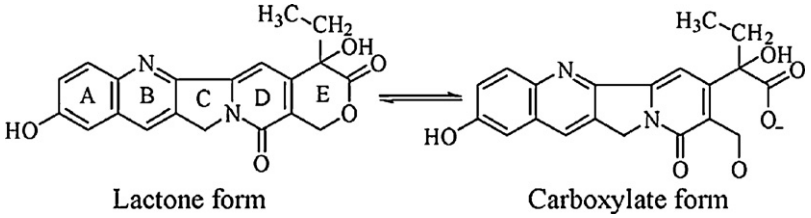

Fig. 1. Conversion of carboxylate form and lactone form of HCPT.

vents. Recently, some research groups begin to investigate the feasibility of polymeric micelle systems. As a promising drug carrier, polymeric micelles (self-assemblies of amphiphilic graft or block copolymers) have attracted a significant attention for the delivery of anti-tumor drugs, due to their special architecture and nano-scale dimension. Polymeric micelles have a core-shell structure composed of hydrophobic segments as the internal core and hydrophilic segments as a surrounding corona in aqueous medium. The hydrophobic core provides a storeroom for hydrophobic drug. The hydrophilic shell allows to the stability of polymeric micelle in aqueous environment, and further modification of the hydrophilic shell can produce properties such as prolonged circulation and specific targeting of the micelles (Hong et al., 2004; Kwon and Okano, 1996). The nano-scale dimensions of polymeric micelles permit their efficient accumulation in tumor tissue via the enhanced permeability and retention (EPR) effect, which is termed as "passive targeting" (Alexis et al., 2008).

Chitosan is a natural polysaccharide derived from chitin by alkaline deacetylation and consists of 2-amino-2-deoxy-(1–4β)-D-glucopyranose residues (D-glucosamine units) and N-acetyl-D-glucosamine units, which is generally regarded as non-toxic, biocompatible and biodegradable. It is widely accepted for a drug delivery carrier. In recent years, many researchers focused on the water soluble chitosan with lower molecular weight, chitosan oligosaccharide (CSO), which had a lower viscosity and better solubility at physiological pH value (7.2–7.4). In our previous researches, the stearic acid grafted chitosan oligosaccharide (CSO-SA) was synthesized by the coupling reaction in the presence of 1-ethyl-3-(3-dimethylaminopropyl) carbodiimide (EDC). The chemical conjugate of CSO-SA could self-aggregate to form micelles in the aqueous phase, and presented an excellent internalization into cancer cells. CSO-SA micelles had been used as the potential carrier for loading anti-tumor drug (Hu et al., 2006a) and efficient gene vector (Hu et al., 2006b). Unfortunately, it was found that it was hard for CSO-SA micelles to encapsulate HCPT because of its bigger molecular weight and rigid structure. Herein, poly (lactic-co-glycolic acid) with carboxylic side group (PLGA) was chosen to be grafted on the backbone additionally by the coupling reaction of carboxyl group of PLGA and amine group of CSO. PLGA has been approved by the FDA for certain human clinical uses (Sahoo et al., 2002) and is widely accepted for pharmaceutical use (Yang et al., 2009). A better encapsulating efficiency and drug loading for HCPT might be realized by the strong hydrophobic interaction between the long chain of PLGA and the molecule of HCPT.

In this research, the stearic acid and poly (lactic-co-glycolic acid) grafted chitosan oligosaccharide (SCP) was obtained by the coupling reaction of carboxyl group of PLGA and SA with amine group of CSO in the presence of 1-ethyl-3-(3-dimethylaminopropyl) carbodiimide (EDC). Properties of SCP micelles, such as the particle size, drug loading, drug encapsulation efficiency and drug release behavior were investigated. In addition, uptake of SCP in tumor cells and cytotoxicity assay were preformed. This study may lead to a novel delivery system for HCPT, and improve the efficacy and safety of its utilization in clinical application.

2. 2 Materials and methods

2.1. Materials

Chitosan (450 kDa, deacetylation degree 95%) was supplied by Yuhuan Marine Biochemistry Co., Ltd., Zhejiang, China. Stearic acid was provided by Shanghai Chemical Reagent Co. Ltd., Shanghai, China. PLGA with carboxylic side group (50:50, M_w: 2000 Da) was purchased from Daigang technology Co. Ltd., Shandong, China. HCPT lyophilized powder was purchased from Xindifu technology Co. Ltd., Xi'an, China. Commercial HCPT injection was purchased from Guizhou Hanfang Pharmaceutical Co., Ltd., Guizhou, China. 2,4,6-trinitrobenzene sulfonic acid (TNBS), 3(4,5-dimethylthiazol-2-yl)-2,5-diphenyl-tetrazolium bromide (MTT), fluorescein isothiocyanate (FITC) and 1-ethyl-3-(3-dimethylaminopropyl) carbodiimide (EDC) were purchased from Sigma (St. Louis, MO, USA). Trypsin and RPMI 1640 Medium were purchased from Gibco BRL, USA. Fetal bovine serum (FBS) was purchased from Sijiqing Biologic, China. All other solvents and reagents were used as chemical or chromatographic grade.

2.2. Synthesis of SA-CSO-PLGA

Firstly, CSO was obtained by enzymatic degradation of chitosan (Hu et al., 2006b, 2008). 25 g of chitosan was dispersed in 750 ml DI water and 9.4 ml of 36.5% (w/v) hydrochloric acid was added. The temperature of the mixture was raised up to 50 °C in batch reactor. With strong agitation, 3% of chitosanase (chitosanase:chitosan = 3%, w/w) was added. The reaction time of hydrolysis was controlled by molecular weight measurement of chitosan performed by gel permeation chromatography (GPC). The temperature of the mixture was raise up to 80 °C to completely inactivate the chitosanase. 0.3% (w/v) activated carbon was added. After agitation, the reaction mixture was then centrifuged for 10 min at 4000 rpm. The obtained supernatant was filtered by filter with 0.45 μm pole size. The low molecular weight chitosan, CSO were obtained by lyophilization (LABCONCO, FreeZone 2.5 Plus, USA).

Secondly, the chemical conjugate of SA-CSO-PLGA was synthesized by the coupling reaction of carboxyl group of PLGA (2 kDa) and SA with amine group of CSO (5 kDa) in the presence of 1-ethyl-3-(3-dimethylaminopropyl) carbodiimide (EDC). Briefly, 0.8 g PLGA, 0.164 g SA and 0.76 g EDC were dissolved in 132 ml acetone aqueous solution (acetone/deionized water = 10/1, v/v). The solution was stirred (250 rpm) for 90 min at 50 °C. One gram of CSO was dissolved in 160 ml deionized water (DI water) and mixed with above acetone solution at 50 °C under stirring. After the coupling reaction was carried out for 24 h, the reaction solution was dialyzed using a dialysis membrane (MWCO: 3.5 kDa, Spectrum Laboratories, Laguna Hills, CA) for 24 h with frequent exchange of DI water to remove by-products and EDC. Finally, dialyzed products were centrifuged at 4000 rpm (3K30, SIGMA Labrorzentrifugen GmbH,Germany) for 10 min to remove un-reacted PLGA and SA. The supernatant was filtered with 0.8 μm water-membrane, and then lyophilized.

2.3. Physicochemical properties of SCP

2.3.1. Micelle size and zeta potential

The average hydrodynamic diameter and zeta potential of SCP micelle solution with 1 mg/ml SCP in distilled water and PBS (pH 7.4) were determined by dynamic light scattering using a Zetasizer (3000HS, Malvern Instruments Ltd., UK).

2.3.2. ^{13}C NMR analysis

SA-CSO-PLGA structure was analyzed by ^{13}C NMR Spectrometer (AC-80, Bruker Biospin, Germany). SCP was dissolved in D_2O with 5 wt%.

2.3.3. Critical micelle concentration (CMC) of SCP

The critical micelle concentrations (CMC) of SCP in DI water and PBS (pH 7.4) were determined by fluorescence measurement using pyrene as a probe (Liu et al., 2007). Pyrene was firstly dissolved in acetone for quantitation. After the acetone was evaporated under 50 °C, 5 ml of SCP solution (DI water or PBS) with different concentrations from 1×10^{-4} to 0.5 mg/ml were added into pyrene. The concentration of pyrene was controlled at 7×10^{-7} M. After the solution was treated by water-bath ultrasonication for 30 min, the fluorescence spectra of solution were measured using fluorometer (F-2500, Hitachi Co., Japan). The excitation wavelength was 334 nm and the slit openings were set at 10 nm (excitation) and 2.5 nm (emission). The pyrene emission was monitored at a wavelength range of 360–450 nm. From the pyrene emission spectra, the intensity ratio of first peak (I_1, 374 nm) to third peak (I_3, 384 nm) was analyzed for the calculation of CMC.

2.3.4. Substitution degree of total amino groups (SD, %) of SCP

The substitute degree of amino groups (SD, %), defined as the number of SA and PLGA groups per 100 amino groups of CSO, was determined by TNBS method (Schnurch and Krajicek, 1998). 2 ml SA-CSO-PLGA solution of DI water with 200 μg/ml SCP were incubated with 2 ml of 4% $NaHCO_3$ and 2 ml of 0.1% TNBS under 37 °C for 2 h. Then, 2 ml of 2 M HCl was added to neutralize the residue of $NaHCO_3$. The ultra-violet (UV) absorbance of samples at 344 nm was measured by UV spectroscopy (TU-1800PC, Beijing Purkinje General Instrument Co., Ltd., China). The SD% of SA-CSO-PLGA was calculated using a calibration curve obtained by the amino-group determination of a series of CSO solutions with different concentrations.

2.4. Preparation and physicochemical characteristics of HCPT-loaded micelle

2.4.1. Preparation of HCPT-loaded micelle (SCP/HCPT)

The HCPT-loaded micelles were prepared by probe-type ultrasonic and dialysis method (Miwa et al., 1998). Briefly, 1 mg/ml SCP solution of DI water and 10 mg/ml HCPT solution in DMSO (HCPT/DMSO) were prepared. 50 or 100 or 200 μl of HCPT/DMSO solution was added into SCP solution (HCPT:SCP = 5%, 10%, 20%, w/w) under mechanical stirring at room temperature for 1 h, then the mixture was treated by probe-type ultrasonic for 90 times in ice-bath (active every 2 s for a 3 s duration, 400 W, JY92-II, Ningbo Xinzhi Scientific Instrument Institute, Zhejiang, China), followed by dialysis against distilled water for 24 h using a membrane with a molecular weight cut-off of 7000 Da. Dialyzed products were centrifuged at 4000 rpm for 10 min to remove precipitated drug during dialysis process. The supernatant was collected to obtain the HCPT-loaded micelles (SCP/HCPT).

2.4.2. Physicochemical characteristics of HCPT-loaded micelle

2.4.2.1. Determination of size and zeta potential of SCP/HCPT. The average hydrodynamic diameter and zeta potential of HCPT-loaded SCP micelle solution (1 mg/ml SCP concentration) in distilled water were determined by dynamic light scattering using a Zetasizer (3000HS, Malvern Instruments Ltd., UK).

2.4.2.2. AFM observation. The morphology and particle size of HCPT-loaded SCP micelles in DI water were observed by an atomic force microscopy (SPA 3800N, SEIKO, Japan). The sample was prepared by casting a dilute micelle solution (1 mg/ml, the aqueous medium with DI water) on a slide glass, which was then in vacuo. Explorer atomic force microscope was a tapping mode, using high resonant frequency (F_0 = 129 kHz), pyramidal cantilevers with silicon probes having force constants of 20 N m^{-1}. Scan speed was set at 2 Hz.

2.4.2.3. Determination of drug entrapment efficiency (EE) and drug loading (DL) of SCP/HCPT. The content of HCPT was measured by HPLC (Agilent1100, Hewlett Packard Co., USA using a Diamohsil™ C_{18} column (200 mm × 4.6 mm, 5 μm particle size). The mobile phase contained acetonitrile, methanol and potassium dihydrogen phosphate solution (0.05 M) with a volume ratio of 60:490:450. The pH was adjusted to 6.4 with 1 M NaOH solution. The HPLC was performed with a flow rate of 0.8 ml/min, a column temperature of 30 °C, and a detection wavelength of 385 nm. The injected volume was 20 μl. Calibration curves with a concentration range of 0.1–10 μg/ml were prepared for both HCPT-lactone and HCPT-carboxylate. All samples were analyzed in triplicate.

To determination of drug entrapment efficiency and drug loading of SCP/HCPT, the HCPT-loaded micelle solution (0.4 ml) was placed into centrifugal-ultrafiltration tube (Microcon YM-10, MWCO 3000, Millipore Co., USA) and centrifuged at 10,000 rpm for 20 min (3K30, SIGMA Labrorzentrifugen GmbH, Germany). The HCPT content in filtrate (C_0, μg/ml) was measured by HPLC. Another 0.4 ml HCPT-loaded micelle solution was diluted 10-fold by methanol aqueous solution (methanol:H_2O = 9:1, v/v) to dissociate the SCP/HCPT micelles. The drug content (C, μg/ml) in diluted solution was also determined. The drug entrapment efficiency and drug loading were then calculated by the following equations:

$$\text{Encapsulation efficiency } (\%) = \frac{(C - C_0) \times V}{M_{\text{drug}}} \times 100\%$$

$$\text{Drug loading content } (\%) = \frac{(C - C_0) \times V}{[W + (C - C_0) \times V]} \times 100\%$$

where M_{drug} represents charged amount of drug and the unit is μg; V represents the total volume of SCP/HCPT micelle solution and the unit is ml; W represents the amount of SCP and the unit is μg.

2.4.2.4. In vitro drug release studies of SCP/HCPT. Sufficient quantum of SCP/HCPT micelle solution with different drug loading (the drug contents were about 50 μg) was added into dialysis membrane (MWCO: 3.5 kDa, Spectrum Laboratories, Laguna Hills, CA) and then placed in plastic tubes with 10 ml of PBS (0.1 M, pH 7.4) solution containing 0.02% (w/v) Tween 80 (Zhang et al., 2007b). The tests were conducted in incubator shaker (HZ-8812S, Scientific and Educational Equipment plant, Tai Cang, China), which was maintained at 37 °C and shaken horizontally at 60 rpm. The dissolution medium was taken at the predetermined time intervals for HPLC analysis, and fresh 10 ml dissolution medium was added into the system. The HCPT solution was test as a control, which was obtained by dissolving 1 mg commercial HCPT lyophilized powder in 10 ml DMSO. All assays were performed in triplicate. The drug content was determined by HPLC method as described above.

2.5. In vitro pharmacodynamics of SCP/HCPT

2.5.1. Cell culture

A549 cells (human lung carcinoma epithelial cell (Alveolar type 2)), MCF-7 (human breast carcinoma cell line) and HepG2 (human hepatocellular carcinoma cell) were maintained in RPMI 1640 supplemented with 10% (v/v) FBS (fetal bovine serum) and penicillin/streptomycin (100 U/ml, 100 U/ml) at 37 °C and 5% CO_2. Cells were sub-cultured regularly using trypsin/EDTA.

2.5.2. Cellular uptake of SCP micelles and SCP/HCPT micelles

2.5.2.1. Preparation of FITC-labeled SCP micelles. FITC-labeled SCP micelles (FITC-SCP) were prepared by dropping ethanol solution of FITC into 1.0 mg/ml of SCP solution. The molar ratio of SCP to FITC was controlled at 1:4. Kept stirring for 24 h with 400 rpm at room temperature in aphotic environment, the reaction product was then dialyzed against DI water using a dialysis membrane (MWCO: 3.5 kDa, Spectrum Laboratories, Laguna Hills, CA) for 24 h to remove the un-reacted FITC.

2.5.2.2. Fluorescence microscope observation. A549, MCF-7 and HepG-2 cells were seeded at 10^5 ml^{-1} cells/well in a 24-well plate (Nalge Nunc International, Naperville, IL, USA) and grown for 24 h, respectively. 50 μl FITC-SCP was added and the cells were further incubated for 1, 6 and 24 h, respectively. After the cells were washed with PBS three times, the cells were observed by fluorescence microscopy (Olympus America, Melville, NY).

2.5.2.3. Determination of intracellular HCPT content. MCF-7 Cells were seeded in a 24-well plate at a seeding density of 10^5 cells/well in 1 ml of growth medium and allowed to attach for 24 h. The cells were then incubated with commercially available HCPT injection and SCP/HCPT (drug concentration: 10 μg/ml) in growth medium for 1, 3, 6, 8 and 12 h. After the cells were washed with PBS three times, 100 μl trypsin PBS solution (2.5 μg/ml) was added. After the further incubation for 5 min, the cells were harvested by adding 400 μl PBS, and then fractured with frost thawing method (Morris et al., 2002). The obtained cell lysate was centrifuged at 10,000 rpm for 10 min. The drug content in the supernatant was measured by HPLC. The protein content in the cell lysate was measured using the micro-BCA protein assay kit. The cellular uptake percentages of drug were calculated from the following equation:

$$\text{Drug uptake percentage } (\%) = \frac{(C/M)}{(C_0/M_0)} \times 100\%$$

where C was intracellular drug concentration in different time, M was unit weight (milligram) of cellular protein in different time, C_0 was initial drug concentration, M_0 was initial unit weight (milligram) of cellular protein.

The recovery tests of HCPT in cells were also carried out. 100 μg/ml O-HCPT and C-HCPT solutions were prepared by dissolving the commercial HCPT powder in 0.1 M NaOH solution and methanol, respectively. 10 μl O-HCPT or C-HCPT solution was added into the harvested cells. The drug content in cells was examined according to the method of the determination of intracellular drug content. The recovery of drug was calculated from the following equation:

$$\text{Recovery of drug} = (C_{\text{O-HCPT}} + C_{\text{C-HCPT}}) \times \frac{0.5\,\text{ml}}{1\,\mu\text{g}} \times 100\%$$

where $C_{\text{O-HCPT}}$ and $C_{\text{C-HCPT}}$ represented the content of O-HCPT and C-HCPT, respectively and the unit was μg/ml.

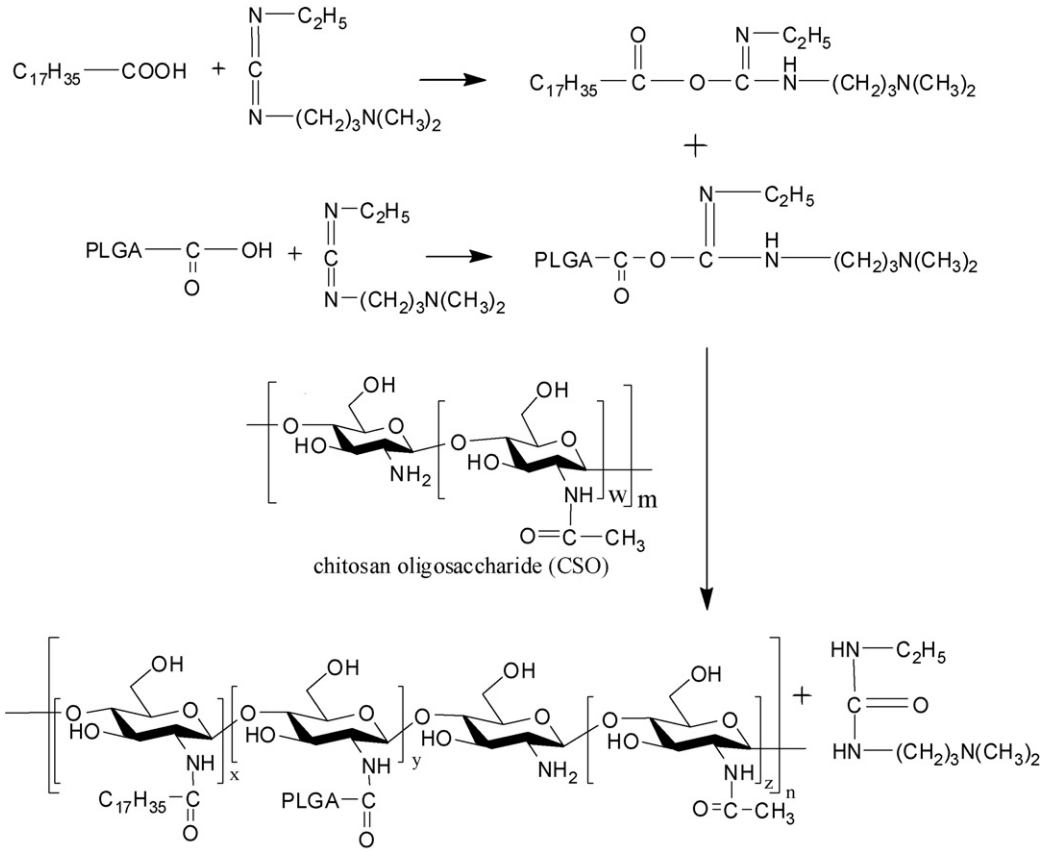

Fig. 2. Synthesis route of the SCP.

Table 1
Characteristics of synthesized SCP.

Micelle	Size by Zave (nm)	PI (–)	Zeta potential (mV)
SA-CSO-PLGA in DI water	396.6 ± 8.6	0.520 ± 0.127	60.6 ± 3.0
SA-CSO-PLGA in PBS (pH 7.4)	451.1 ± 0.6	0.246 ± 0.162	11.3 ± 3.2

PI: Polydispersity Index.

2.5.3. Cytotoxicity assay

Cytotoxicitys of SCP micelles, HCPT injection and SCP/HCPT against A549, MCF-7 and HepG2 cells were evaluated by MTT assay (Zhang et al., 2007c). The cells were seeded at 1.0×10^5 ml^{-1} cells/well in a 96-well plate (Nalge Nunc International, Naperville, IL, USA) and grown for 24 h. The solution of SA-CSO-PLGA, HCPT inject, SCP/HCPT with different concentrations was added, respectively. The cells were incubated for further 48 h. 20 μl MTT solution (5 mg/ml in DI water) was then added to each well. After 4 h further incubation, the culture medium was removed, and the formazan crystals in cells were solubilized with 200 μl DMSO for 15 min. The UV absorbance at 570 nm was measured using a microplate reader (Bio-Rad, Model 680, USA.).

2.6. Conversion of O-HCPT and C-HCPT of HCPT under different pH

To study the stability of lactone ring of HCPT in different pH condition, commercial HCPT powder was dissolved in the 0.02 mM buffered phosphate solution with diferent pH values (5.0, 5.6, 6.5, 7.0, 7.4, 7.8, 9.0). The HCPT solution were incubated in incubator shaker (HZ-8812S, Scientific and Educational Equipment plant, Tai Cang, China), which was maintained at 37 °C and shaken horizontally at 60 rpm for 72 h (Zhou et al., 2001). The liquid was then centrifugated at 4000 rpm (3K30, SIGMA Labrorzentrifugen GmbH,Germany) for 10 min to remove precipitated drug and the supernatant was filtered with 0.45 μm water-membrane. The filtrate was measured by HPLC to calculate the ratio of O-HCPT and C-HCPT.

2.7. Stability of SCP/HCPT micelles

The drug-loaded micelle solution was kept in a sealed flask at 4 °C for 2 months. The encapsulation efficiency and the HCPT loading were examined again by HPLC method. Furthermore, the micellar size and Zeta potential were also measured using a Zetasizer 3000HS instrument.

3. Results and discussions

3.1. Synthesis of SCP

The low molecular weight chitosan was obtained by enzymatic degradation of chitosan and the molecular weight of the final obtained CSO was measured by gel permeation chromatography (Hu et al., 2006b). The Mw (weight average molecular weight) of CSO used in this paper was about 5 kDa. The obtained CSO could be easily dissolved in physiological pH aqueous medium. In our previous study, the chemical conjugate of CSO-SA could self-aggregate to form micelles in the aqueous phase, and presented an excellent internalization into cancer cells. But it was also found that it was hard for CSO-SA micelles to encapsulate HCPT because of its bigger molecular weight and rigid structure. PLGA was chosen to be grafted on the backbone additionally by the coupling reaction of carboxyl group of PLGA and amine group of CSO. It had an open structure as the hydrophobic segment, which would make HCPT enter the core of micelles easily. In the presence of EDC, carboxyl groups of SA and PLGA formed an active intermediate and easily reacted with the primary amino groups of CSO to generate the final SCP. The synthesis route of SCP was shown in Fig. 2. The synthesized SCP owned amphipathic properties and could easily self-aggregate into nano-scale structure in aqueous environment because of the hydrophilic CSO chains and the hydrophobic SA and PLGA chains, which composed the internal hydrophobic core and the surrounding hydrophilic shell, respectively. The hydrophobic core could not only provide a space for hydrophobic drugs to enhance the solubility of drug in physiological environment, but also protect the drugs from degradation or degenerescence. Meanwhile, the hydrophilic shell was able to allow polymeric micelles gain the stability in aqueous environment.

The total substitute degree of amino groups (SD %) of SCP by SA and PLGA was measured by the TNBS method. TNBS is a substance that can react with the remaining primary amino residues of the CSO molecules. The absorbance of the purple reaction production could be determined by a UV spectrophotometer. The SD % of SCP was determined as (13.96 ± 0.17)%.

The structure of obtained SCP was confirmed by ^{13}C NMR spectrum (Fig. 3). The peaks at 179 and 180 ppm were attributed to the carbonyl carbons of grafted PLGA of SCP; the peak at about 174 ppm was attributed to the carbonyl carbons of stearate group of SCP. The other peaks were mainly attributed to the chitosan oligosaccharide of SCP and alkyl groups of SA. These results demonstrated that the SA and PLGA were successfully grafted onto the chitosan chains. According to the area of the peaks, the molar ratio of grafted PLGA and SA was then calculated as 1:1.4, thus the substitution degree of SA and PLGA were 8.15% and 5.82%, respectively.

3.2. Characteristics of SCP micelles

The size and zeta potential of SCP micelles with 1.0 mg/ml SCP concentration in DI water and PBS (pH 7.4) were shown in Table 1. The *Z*-average size in DI water and PBS were 396.6 and 451.1 nm, respectively. Furthermore, the SCP had a high positive potential about 60.6 mV in DI water, which indicated the micelle could be stable in the water. Influenced by the decreased protonation of amino groups of CSO in higher pH condition, zeta potential of SCP in PBS (pH 7.4) decreased to 11.3 mV.

The critical micelle concentration (CMC) of SCP in DI water and PBS (pH 7.4) was determined by fluorescence spectroscopy using pyrene as a probe. In the lower SCP concentration, the intensity ratio of the first energy band (374 nm, I_1) to the third energy band (384 nm, I_3) of the pyrene emission spectra kept a constant. When the micelles formed, the incorporation of pyrene into the

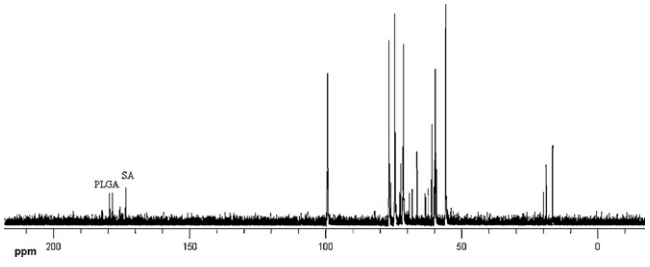

Fig. 3. ^{13}C NMR spectrum of SCP.

Table 2
Characteristics of SCP/HCPT micelles.

Sample	Size by Zave (nm)	PI (–)	Zeta potential (mV)	DL (%)	EE (%)
5%	240.8 ± 4.8	0.254 ± 0.062	40.7 ± 0.3	4.71 ± 0.14	97.50 ± 2.11
10%	265.8 ± 5.2	0.220 ± 0.046	38.6 ± 0.1	8.74 ± 0.37	95.76 ± 3.20
20%[a]	315.1 ± 7.4	0.176 ± 0.021	38.5 ± 0.5	14.77 ± 0.23	86.65 ± 1.12
20%[b]	315.2 ± 8.3	0.204 ± 0.052	37.8 ± 2.6	14.68 ± 0.52	86.06 ± 2.43

PI: Polydispersity Index.
[a] Represents fresh HCPT-loaded SA-CSO-PLGA micelles
[b] Represents HCPT-loaded SA-CSO-PLGA micelles after 2 months.

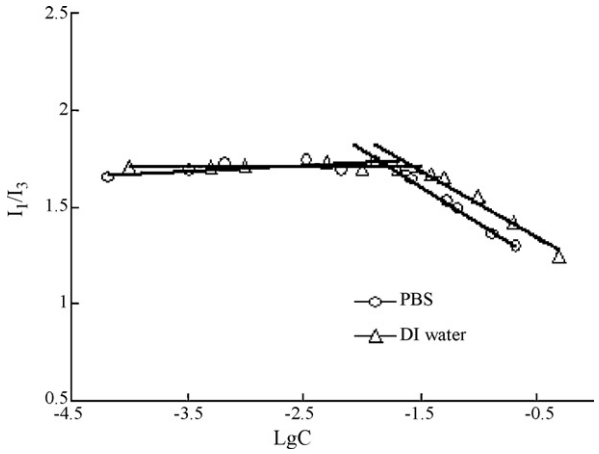

Fig. 4. Variation of fluorescence intensity ratio for I_1/I_3 against logarithm of SCP concentration.

micelles led to the increase of fluorescence intensity. The I_3 of pyrene increased more significantly than that of I_1. As a result, the fluorescence intensity ratio of I_1/I_3 was reduced. Fig. 4 shows the variation of fluorescence intensity ratio for I_1/I_3 against the logarithm of SCP concentration. The concentration corresponding to the break point in Fig. 4 was the CMC value of SCP. The CMC values of SCP in DI water and in PBS (pH 7.4) were 34.9 and 14.5 μg/ml, respectively. The lower CMC of SCP in PBS might be due to decrease of electrostatic repulsion between SCP molecules. Because the pKa of chitosan was about 6.5, the protonation of amino groups of CSO in PBS was poorer than that in DI water. Consequently, the zeta potential and electrostatic repulsion of SCP in PBS decreased. This result made the SCP form micelles more easily with a lower CMC in PBS, of which the pH value was closed to that of body fluid (Rapoport, 1999).

3.3. Characteristics of SCP/HCPT

HCPT-loaded SCP micelles with different charged ratios of HCPT were prepared by the probe-type ultrasonic and dialysis method. The properties, such as micelle size, zeta potential, EE and DL of SCP/HCPT were shown in Table 2. The size of SCP/HCPT was smaller than that of blank SCP micelle (Table 2), and slightly increased from 240.8 to 315.2 nm when the charged ratio of HCPT increased from 5% to 20%. This might be due to the increase of cohesive force after drug loading into the hydrophobic region. It was also found that the zeta potentials were reduced after the drug was loaded. However, there were above 30 mV, and had no significant difference between the zeta potentials of HCPT-loaded SCP micelles with different charged ratios of HCPT. The positive potential in the surface could facilitate the cellular uptake of nanoparticles (Tahara et al., 2009).

Fig. 5 showed the AFM images of the HCPT-loaded SCP micelles. AFM is a powerful tool for detecting the size and surface morphology of micelles. The claviform morphologies of HCPT-loaded SCP micelles were confirmed from AFM images. It was found the micelles size observed from AFM was smaller than that obtained from DLS determination. It might be due to the shrink of hydrophilic backbone in the micelles during the dry process of AFM sample.

EE and DL of SCP/HCPT were determined by HPLC method. As shown in Table 2, SCP/HCPT had a high EE. It was clear that when the charged ratio of HCPT increased from 5% to 20%, the EE of SCP/HCPT decreased gradually, but DL enhanced noticeably. When 20% HCPT was charged, the DL of SCP/HCPT could reach up to 14.77%. It is well known that DL and EE are two important characters of the micellar system. It depends on several factors, such as chemical constitution of polymer micelle and drug, charged amount of drugs and the ratio of aqueous phase to organic phase during the preparation process (Zhang et al., 2007b). It is usually hard to entrap hydrophobic anticancer drugs because of their big molecular weight and rigid structure as we known. The high EE of SCP for HCPT might be related

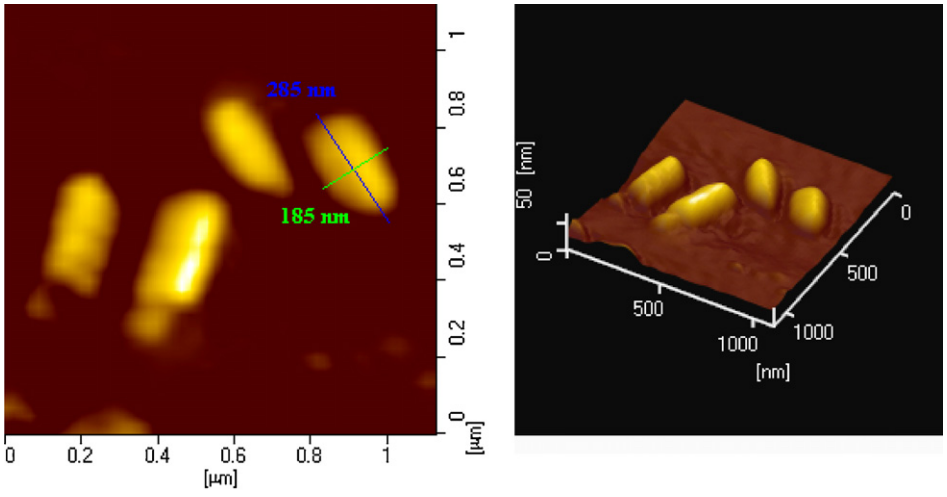

Fig. 5. AFM images of HCPT-loaded micelles.

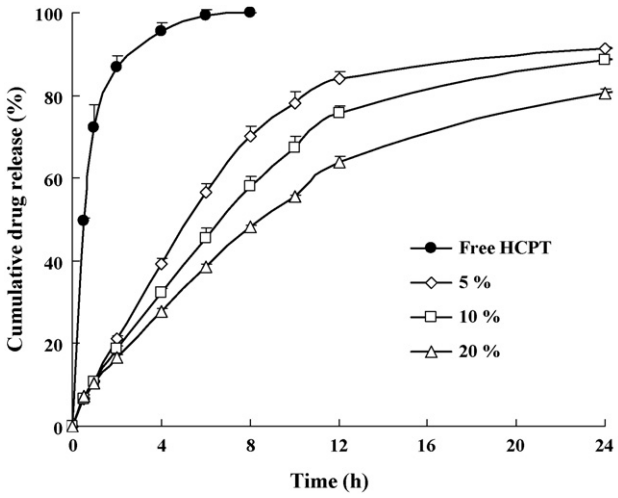

Fig. 6. In vitro release of HCPT from HCPT-loaded micelles.

to the PLGA on backbone of SCP. PLGA had a long molecular chain and an open structure as the hydrophobic segment, which made HCPT enter the core of micelles easily.

In vitro HCPT release from SCP/HCPT micelles with different charged drug ratios (5%, 10%, 20%) was carried out using PBS (pH 7.4) containing 0.02% (w/v) Tween 80 as a dissolution medium. Fig. 6 shows the drug release profiles from SCP/HCPT. Free HCPT had released 90% in 4 hour and completely released in 8 h. But there was no obvious burst releasing of HCPT from SCP/HCPT, and it took about 5–9 h to release 50% of the drug-loaded, and final cumulative drug release percent achieved 80–90% in 24 h. This result may be attributed to the very slow diffusion of HCPT from the SCP micelles but not a simple penetration of drug molecules through the dialysis membrane. Furthermore, the sustained-release behavior was more significant with the increase of charged ratio of drug.

Table 3
IC_{50} of SA-SCP-PLGA, HCPT injection, SCP/HCPT against A549, MCF-7 and HepG2.

Cell lines	HCPT injection (μg/ml)	SCP/HCPT (μg/ml)	Reduced fold (–)
MCF-7	30.3 ± 2.1	1.7 ± 0.7	18
HepG-2	2.0 ± 0.5	0.1 ± 0.1	15
A549	56.6 ± 13.3	2.3 ± 0.6	22

3.4. Pharmacodynamics of SCP/HCPT in cells

The cellular inhibition of blank SCP at concentration of 100 μg/ml was less than 20% against A549, MCF-7 and HepG2 cells. It suggested that the material showed a low cytotoxicity. The cytotoxicity results of SCP/HCPT and HCPT injection against A549, MCF-7 and HepG2 cell lines were shown in Table 3. There was a sharp discrimination in IC_{50} between the commercial HCPT injection and SCP/HCPT. The IC_{50} of SCP/HCPT was about 15–22 times lower than that of HCPT injection, which indicated that HCPT-loaded micelles presented a significantly enhanced cytotoxicity against the tested tumor cell lines. It might be caused by two factors. Firstly, commercial HPCT injection was prepared by NaOH. Almost all of the HCPT existed as a form of O-HCPT because of the higher pH, but HCPT in the micelles was still in the form of C-HCPT. As was reported, the cytotoxicity of C-HCPT was much better than that of O-HCPT. Secondly, the intracellular drug content increased because of the transport of SCP. The variance of IC_{50} against A549, MCF-7 and HepG2 might result from the different amount of Topo-I in cells. The IC_{50} of HCPT injection and HCPT/SCP towards HepG2 were much smaller compared with the other cell lines, which were 2.0 and 0.1 μg/ml, respectively.

Fig. 7 showed fluorescent microscopic images of co-cultured A549, MCF-7 and HepG-2 cells with FITC-labeled SCP for 1, 6 and 24 h, respectively. It was clear that the cellular uptake of SCP was increased with the incubation time. However, there was no obvious difference between A549, MCF-7 and HepG-2. The micelles presented an excellent cellular internalization, which might be

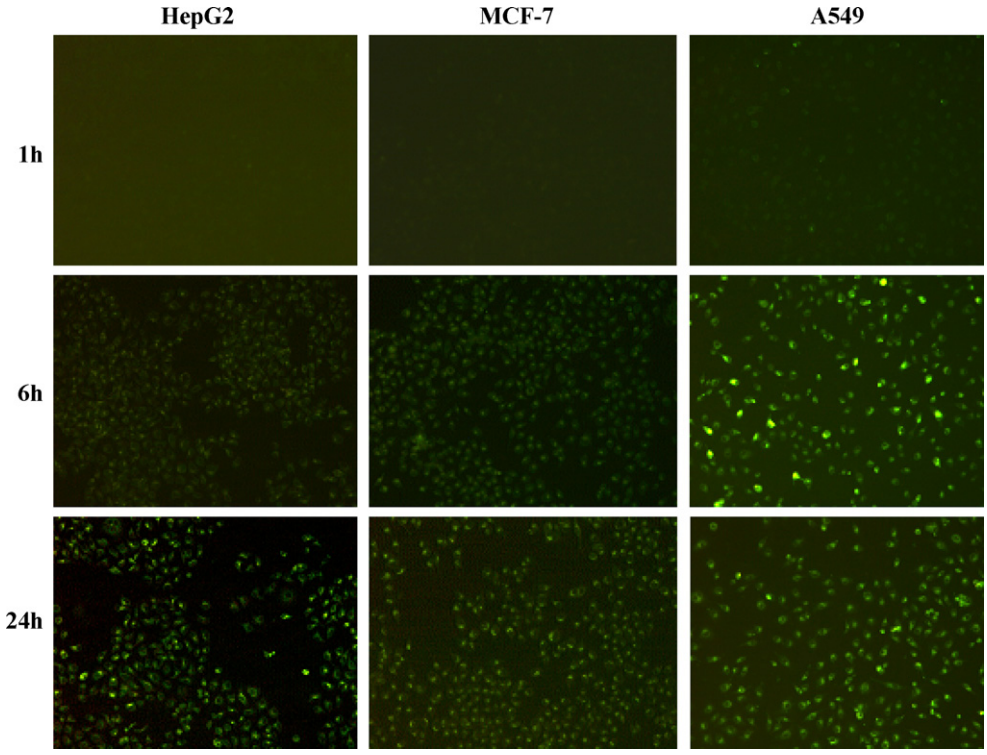

Fig. 7. Fluorescent microscopy images of co-cultured A549, MCF-7 and HepG-2 cells with FITC-labled SCP for different time.

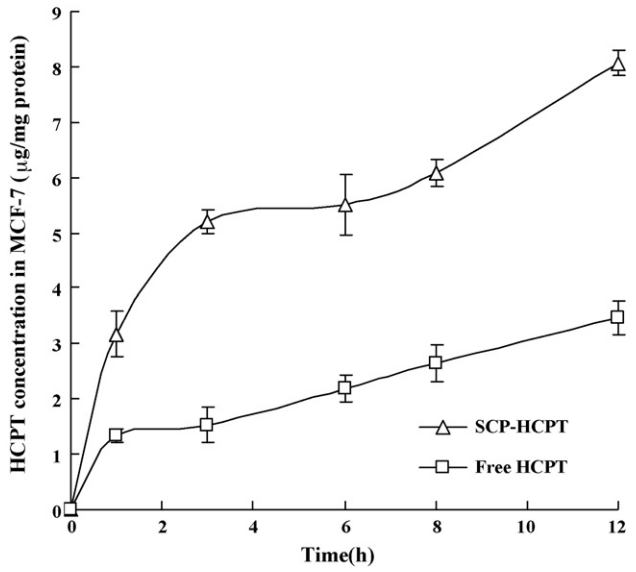

Fig. 8. Variation of concentration of HCPT in MCF-7 against the incubation time.

due to their special spatial structure and glycolipid-like components (Hu et al., 2008). In addition, the excellent internalization of SCP micelles enhanced the cellular uptake of drug-loaded micelles, made the drug release inside the cells, which could protect the drug from conversion before arriving at the tumor cells and improve the anti-tumor effect of HCPT.

The intracellular drug content was further determined. At first, the recovery of HCPT in cells was conducted. The recovery of O-HCPT and C-HCPT were 96.3–101.9% and 95.4–103.1%, respectively. It demonstrated that there was no influence of the experimental procedure to the determination of HCPT. In addition, because of the influence of pH value, 73.3% C-HCPT changed into O-HCPT and 23.67% O-HCPT changed into C-HCPT as well.

Fig. 8 showed the intracellular HCPT content after the HCPT injection and SCP/HCPT were incubated with MCF-7 cells. The cellular uptake of HCPT in SCP/HCPT was faster than that of HCPT injection and the total uptake drug amount of SCP/HCPT was about twice increased, which indicated that the drug amount in cells was successfully enhanced through the encapsulating by SCP micelles. As a result, the anti-tumor effect could be improved.

3.5. Stability of HCPT in SCP/HCPT

It was widely reported that the integrity of the lactone ring of HCPT was required for both passive diffusion into cancer cells and suppressing topoisomerase I activity (Burke and Mi, 1994).

It is a pity that C-HCPT can easily transform into O-HCPT in high pH value. Furthermore, O-HCPT has little anti-tumor activity, but a potential toxicity. The influence of pH to the conversion between O-HCPT and C-HCPT were investigated. As shown in Fig. 9, the retention times of the O-HCPT and C-HCPT under the HPLC analytical conditions were 5.6 and 8.9 min, respectively. As shown in Fig. 10, HCPT existed as the form of C-HCPT when the pH was below 5.5. The ratio of C-HCPT to O-HCPT decreased with the increasing pH. In physiological condition (pH 7.4), the ratio was about 21%. When the pH was above 9.0, HCPT exited as the form of O-HCPT. The commercial HCPT injection was a NaOH solution with the pH value about 9.0, which indicated that the HCPT mostly was the O-HCPT. That is why the dosage is so huge in clinic but the anti-tumor effect is poor relatively.

In the determination tests of EE and DL for SCP/HCPT, it was found that the retention time of the HCPT in micelles extracted by

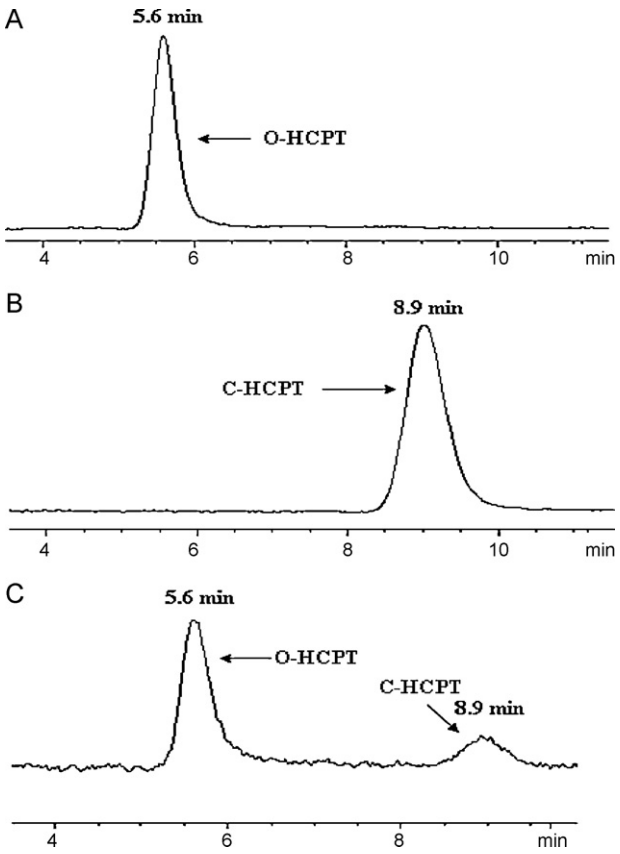

Fig. 9. HPLC analysis of HCPT: (A) HCPT in 0.1 mol/l NaOH solution; (B) HCPT in methanol; (C) HCPT in PBS (pH 7.4).

methanol was 8.9 min, which demonstrated that it existed as the form of C-HCPT. After the C-HCPT molecule was entrapped into the hydrophobic core of SCP micelles, the lactone ring of HCPT was isolated from aqueous environment. Thus, C-HCPT would not transform into O-HCPT because of pH value. The micelles showed an important protection for C-HCPT.

After the SCP/HCPT solution was kept in a sealed flask at 4 °C for 2 months, the micellar size, Zeta potential, encapsulation efficiency and the HCPT loading capacity were examined again. Compared to the fresh HCPT-loaded micelles, there was no significant change in these properties, which suggested that the SCP/HCPT was stable, and the SCP micelle could be used as a carrier of HCPT (Table 2).

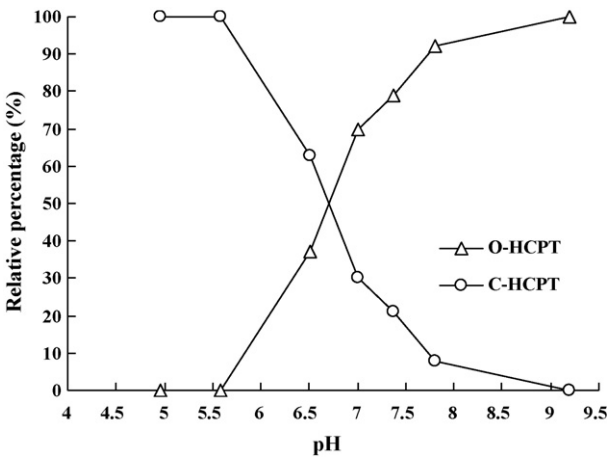

Fig. 10. Conversion between O-HCPT and C-HCPT under different pH.

4. Conclusions

The chemical conjugate of SA-CSO-PLGA was successfully synthesized. Lower CMC, high HCPT encapsulation efficiency and the loading capacity, and the enhanced drug stability of SA-CSO-PLGA micelles presented an excellent candidate for a drug delivery carrier. Furthermore, the cellular internalization of drug-loaded SA-CSO-PLGA micelles also improved the anti-tumor effect of HCPT. The SA-CSO-PLGA micelles would be expected as a carrier for the hydrophobic HCPT.

Acknowledgments

We are grateful for financial support of National Basic Research Program of China (973 Program) under contract 2009CB930300, National HighTech Research and Development Program (863) of China (2007AA03Z318), and Foundation of Science and Technology Department of Zhejiang Province (2008C23043).

References

Alexis, K., Pridgen, E., Molnar, L.K., Farokhzad, O.C., 2008. Factors affecting the clearance and biodistribution of polymeric nanoparticles. Mol. Pharm. 5, 505–515.
Burke, T.G., Mi, Z., 1994. The structural basis of camptothecin interactions with human serum albumin impact on drug stability. J. Med. Chem. 37, 40–46.
Carbonero, R., Supko, J.G., 2002. Current perspectives on the clinical experience,pharmacology, and continued development of the camptothecins. Clin. Cancer Res. 8, 641–661.
Cortesi, R., Esposito, E., Maietti, A., Menegatti, E., Nastruzzi, C., 1997. Formulation study for the antitumor drug camptothecin: liposomes, micellar solutions and a microemulsion. Int. J. Pharm. 159, 95–103.
Ertl, B., Platzer, P., Wirth, M., Gabor, F., 1999. Poly(D,L-lactic-co-glycolic acid) microspheres for sustained delivery and stabilization of camptothecin. J. Control. Release 61, 305–317.
Guo, R., Zhang, L.Y., Jiang, Z.P., Cao, Y., Ding, Y., Jiang, X.Q., 2007. Synthesis of alginic acid-poly[2-(diethylamino)ethyl methacrylate] monodispersed nanoparticles by a polymer-monomer pair reaction system. Biomacromolecules 8, 843–850.
Han, R., 1994. Highlight on the studies of anticancer drugs derived from plants in China. Stem Cells 12, 53–63.
He, X.G., Lu, W., Jiang, X.Q., Zhang, X.W., Ding, J., 2004. Synthesis and biological evaluation of bis and monocarbonate prodrugs of 10-hydroxycamptothecins. Bioorg. Med. Chem. 12, 4003–4008.
Hong, J.W., Park, J.H., Huh, K.M., Chung, H., Kwon, I.C., Jeong, S.Y., 2004. PEGylated polyethylenimine for in vivo local gene delivery based on lipiodolized emulsion system. J. Control. Release 99, 167–176.
Hong, M.H., Zhu, S.J., Jiang, Y.Y., Tang, G.T., Pei, Y.Y., 2009. Efficient tumor targeting of hydroxycamptothecin loaded PEGylated niosomes modified with transferrin. J. Control. Release 133, 96–102.
Hu, F.Q., Ren, G.F., Yuan, H., Du, Y.Z., Zeng, S., 2006a. Shell cross-linked stearic acid grafted chitosan oligosaccharide self-aggregated micelles for controlled release of paclitaxel. Colloids Surf. B 50, 97–103.
Hu, F.Q., Wu, X.L., Du, Y.Z., You, J., Yuan, H., 2008. Cellular uptake and cytotoxicity of shell crosslinked stearic acid-grafted chitosan oligosaccharide micelles encapsulating doxorubicin. Eur. J. Pharm. Biopharm. 69, 117–125.
Hu, F.Q., Zhao, M.D., Yuan, H., You, J., Du, Y.Z., Zeng, S., 2006b. A novel chitosan oligosaccharide–stearic acid micelles for gene delivery: properties and in vitro transfection studies. Int. J. Pharm. 315, 158–166.
Kwon, G.S., Okano, T., 1996. Polymeric micelles as new drug carriers. Adv. Drug Deliv. Rev. 21, 107–116.
Laco, G.S., Collins, J.R., Luke, B.T., Kroth, H., Sayer, J.M., Jerina, D.M., Pommier, Y., 2002. Human topoisomerase I inhibition: docking camptothecin and derivatives into a structure-based active site model. Biochemistry 41, 1428–1435.
Liu, S.Q., Wiradharma, N., Gao, S.J., Tong, Y.W., Yang, Y.Y., 2007. Bio-functional micelles self-assembled from a folate-conjugated block copolymer for targeted intracellular delivery of anticancer drugs. Biomaterials 28, 1423–1433.
Lu, B., Zhang, Z.Q., 2006. Novel colon-specific microspheres with highly dispersed hydroxycamptothecin cores: their preparation, release behavior, and therapeutic efficiency against colonic cancer. J. Pharm. Sci. 95, 2619–2630.
Miwa, A., Ishibe, A., Nakano, M., Yamahira, T., Itai, S., Jinno, S., Kawahara, H., 1998. Development of novel chitosan derivatives as micellar carriers of taxol. Pharm. Res. 15, 1844–1850.
Morris, J.D., Fernandez, J.M., Chapa, A.M., Gentry, L.R., Thorn, K.E., Weick, T.M., 2002. Effects of sample handling, processing, storage, and hemolysis on measurement of key energy metabolites in ovine blood. Small Ruminant Res. 43, 157–166.
Muggia, F.M., Creaven, P.J., Hansen, H.H., Cohen, M.H., Selawry, O.S., 1972. Phase I clinical trials of weekly and daily treatment withcamptothecin. Cancer Chemother. Rep. 56, 515–521.
O'Leary, J., Muggia, F.M., 1998. Camptothecins: a review of their development and schedules of administration. Eur. J. Cancer 34, 1500–1508.
Pourquier, P., Pommier, Y., 2001. Topoisomerase I-mediated DNA damage. Adv. Cancer Res. 80, 189–216.
Rapoport, N., 1999. Stabilization and activation of Pluronic micelles for tumor-targeted drug delivery. Colloid Surf. B: Biointerfaces 16, 93–111.
Sahoo, S.K., Panyam, J., Prabha, S., Labhasetwar, V., 2002. Residual polyvinyl alcohol associated with poly(D,L-lactide-co-glycolide) nanoparticles affects their physical properties and cellular uptake. J. Control. Release 82, 105–114.
Schnurch, A.B., Krajicek, M.E., 1998. Mucoadhesive polymers as platforms for peroral peptide delivery and absorption: synthesis and evaluation of different chitosan-EDTA conjugates. J. Control. Release 50, 215–223.
Shenderova, A., Burke, T.G., Schwendeman, S.P., 1999. The acidic microelimate in poly(lactide-co-glycolide) microspheres stabilizes camptothecins. Pharm. Res. 16, 241–248.
Shenderova, A., Burke, T.G., Sehwendeman, S.P., 1997. Stabilization of 10-hydroxycamptothecin in poly (lactide-co-glycolide) microsphere delivery vehicles. Pharm. Res. 14, 1406–1414.
Shi, B., Fang, C., Pei, Y.Y., 2006. Stealth PEG-PHDCA niosomes: effects of chain length of peg and particle size on niosomes surface properties, in vitro drug release, phagocytic uptake, in vivo pharmacokinetics and antitumor activity. J. Pharm. Sci. 95, 1873–1887.
Sun, X., Wu, F., Lu, W., Zhang, Z.R., 2004. Sustained-release hydroxycamptothecin polybutylcyanoacrylate nanoparticles as a liver targeting drug delivery system. Pharmazie 59, 791–794.
Tahara, K., Yamamoto, K., Hirashima, N., Kawashima, Y., 2009. Chitosan-modified poly (D,L-lactide-co-glycolide) nanospheres for improving siRNA delivery and gene-silencing effects. Eur. J. Pharm. Biopharm., doi:10.1016/j.ejpb.2009.12.007.
Thomas, C.J., Rahier, N.J., Hecht, S.M., 2004. Camptothecin: current perspectives. Bioorg. Med. Chem. 12, 1585–1604.
Tsao, Y.P., Russo, A., Nyamuswa, G., Silber, R., Liu, L.F., 1993. Interaction between replication forks and topoisomerase-I-DNA cleavable complexes: studies in a cell-free SV40 DNA replication system. Cancer Res. 53, 5908–5914.
Wall, M.E., Wani, M.C., Cook, C.E., Palmer, K.H., McPhail, A.T., Sim, G.A., 1966. Plant antitumor agents. I. isolation and structure of camptothecin, a novel alkaloidal leukemia and tumor inhibitor from Camptotheca acuminate. J. Am. Chem. Soc. 88, 3888–3890.
Wang, Y.Q., Li, L.F., Jiang, W., Larrick, J.W., 2005. Synthesis and evaluation of a DHA and 10-hydroxycamptothecin conjugate. Bioorg. Med. Chem. 13, 5592–5599.
Wani, M.C., Ronman, P.E., Lindley, J.T., Wall, M.E., 1980. Plant antitumor agents.18. Synthesis and biological activity of camptothecin analogues. J. Med. Chem. 23, 554–560.
Yang, L., Cui, F.D., Cun, D.M., Tao, A.J., Shi, K., Lin, W.H., 2007. Preparation, characterization and biodistribution of the lactone form of 10-hydroxycamptothecin (HCPT)-loaded bovine serum albumin (BSA) nanoparticles. Int. J. Pharm. 340, 163–172.
Yang, R., Shim, W.S., Cui, F.D., Cheng, G., Han, X., Jin, Q.R., Kim, D.D., Chung, S.J., Shim, C.K., 2009. Enhanced electrostatic interaction between chitosan-modified PLGA nanoparticle and tumor. Int. J. Pharm. 371, 142–147.
Zhang, J.A., Xuan, T., Parmar, M., Ma, L., Ugwu, S., Ali, S., Ahmad, I., 2004. Development and characterization of a novel liposome-based formulation of SN-38. Int. J. Pharm. 270, 93–107.
Zhang, R.W., Li, Y.F., Cai, Q.Y., Liu, T.P., Sun, H., Chambless, B., 1998. Preclinical pharmacology of the natural product anticancer agent 10-hydroxycamptothecin, an inhibitor of topoisomerasc I. Cancer Chemother. Phammcol. 41, 257–267.
Zhang, L.Y., Sun, M.J., Guo, R., Jiang, Z.P., Liu, Y., Jiang, X.Q., Yang, C.Z., 2006. Chitosan surface-modified hydroxycamptothecin loaded nanoparticles with enhanced transport across Caco-2 cell monolayer. J. Nanosci. Nanotechnol. 6, 2912–2920.
Zhang, L.Y., Yang, M., Wang, Q., Li, Y., Guo, R., Jiang, X.Q., Yang, C.Z., Liu, B.R., 2007a. 10-Hydroxycamptothecin loaded nanoparticles: preparation and antitumor activity in mice. J. Control. Release 119, 153–162.
Zhang, C., Ding, Y., Liangli (Lucy), Yu, Ping, Q.N., 2007b. Polymeric micelle systems of hydroxycamptothecin based on amphiphilic N-alkyl-N-trimethyl chitosan derivatives. Colloids Surf. B: Biointerfaces 55, 192–199.
Zhang, Y.D., Hu, Z.Y., Ye, M.Y., Pan, Y.F., Chen, J.J., Luo, Y.L., Zhang, Y.Q., He, L.X., Wang, J.W., 2007c. Effect of poly(ethylene glycol)-block-polylactide nanoparticles on hepatic cells of mouse: low cytotoxicity, but efflux of the nanoparticles by ATP-binding cassette transporters. Eur. J. Pharm. Biopharm. 66, 268–280.
Zhao, Y.X., Gao, J.Q., Sun, X.Y., Chen, H.L., Wu, L.M., Liang, W.Q., 2007. Enhanced nuclear delivery and cytotoxic activity of hydro-xycamptothecin using o/w emulsions. J. Pharm. Pharm. Sci. 10, 61–70.
Zhou, J.J., Liu, J., Xu, B., 2001. Relationship between lactone ring forms of HCPT and their antitumor activities. Acta Pharmacol. Sin. 22, 827–830.